

D-Glucose-induced Dysmorphogenesis of Embryonic Kidney

Yashpal S. Kanwar,* Zheng Z. Liu,* Anil Kumar,* M. Irtaza Usman,* Jun Wada,* and Elisabeth I. Wallner[‡]

*Department of Pathology, and [‡]Department of Medicine, Northwestern University Medical School, Chicago, Illinois 60611

Abstract

An organ culture system was used to study the effect of D-glucose on embryonic kidneys, and to delineate the mechanism(s) relevant to their dysmorphogenesis. Metanephroi were cultured in the presence of 30 mM D-glucose. A notable reduction in the size and population of nephrons was observed. Ureteric bud branches were rudimentary and the acuteness of their tips, the site of nascent nephron formation, was lost. Metanephric mesenchyme was atrophic, had reduced cell replication, and contained numerous apoptotic cells. Competitive reverse transcriptase-PCR analyses and immunoprecipitation studies indicated a decrease in expression of heparan sulfate proteoglycan (perlecan). Status of activated protein-2 was evaluated since its binding motifs are present in the promoter region of the perlecan gene. Decreased binding activity of activated protein-2, related to its phosphorylation, was observed. D-glucose-treated explants also had reduced levels of cellular ATP. Exogenous administration of ATP restored the altered metanephric morphology and reduced [³⁵S]sulfate-incorporated radioactivity associated with perlecan. The data suggest that D-glucose adversely affects the metanephrogenesis by perturbing various cellular phosphorylation events involved in the transcriptional and translational regulation of perlecan. Since perlecan modulates epithelial/mesenchymal interactions, its deficiency may have led to the metanephric dysmorphogenesis and consequential atrophy of the mesenchyme exhibiting accelerated apoptosis. (*J. Clin. Invest.* 1996, 98:2478–2488.)
Key words: kidney development • diabetes • apoptosis • proteoglycans • adenosine triphosphate

Introduction

Diabetes mellitus is a common metabolic disorder in which the hyperglycemic state seems to adversely affect the homeostasis of various organ systems, including the kidney (1, 2). The pathologic changes of the kidney are characterized by biochemical alterations of the extracellular matrix (ECM)¹ macromolecules; the latter are believed to regulate morphogenesis of different organ systems (3, 4). In this regard, a significant increase in the congenital defects, involving multiple organs, in the offsprings of poorly controlled juvenile diabetic mothers

have been described (5–9). The congenital defects include failure in the closure of neural tube, caudal regression syndrome, and genito-urinary abnormalities, including agenesis of the kidney. Similarly, an increased incidence of congenital defects has been observed in the offsprings of alloxan- and streptozotocin-induced diabetic rats and mice (10–14), and also in non-obese diabetic mice (15). In embryos of these murine diabetic mothers, changes in some of the ECM macromolecules (16), altered mitochondrial morphology of the anterior neuropore (17), perturbed phosphorylation or dephosphorylation processes relevant to the tyrosine kinase activities of growth factor receptors (18, 19), and metabolism of myo-inositol (20) have been described. In addition, certain other mechanisms (e.g., free oxygen radical-induced injury, reference 21), may also be relevant in the pathogenesis of hyperglycemia-induced embryopathy. The induction of such embryonic defects and the mechanisms involved have been further investigated in whole rat embryo culture systems (22, 23). Exposure of rat embryos, harvested during the midgestational period, to elevated concentrations of aldohexoses (i.e., glucose, fructose, mannose, and galactose) for 3–4 d results in the development of complex abnormalities confined to the lower half of the body; e.g., non-closure of the neural tube (13, 14, 23). These extensive *in vivo* as well as *in vitro* studies, carried out over a period of 2–3 decades, strongly suggest a significant correlation between the hyperglycemic state and abnormal development of the mammalian embryo. However, available data concerning the dysmorphogenetic effect of hyperglycemia on the individual embryonic organ system, (e.g., metanephros) are rather limited.

The mammalian metanephros develops by cranial migration of the ureteric bud, followed by reciprocal interaction of its epithelia with the undifferentiated mesenchyme (24). During these interactions, a number of protooncogenes, growth factors, ECM macromolecules, and their receptors regulate metanephric morphogenesis that involves the differentiation of mesenchyme into glomerular and tubular elements of the kidney (25, 26). Of particular interest are the ECM macromolecules, especially the proteoglycans (PGs), which are present at the epithelial/mesenchymal interface and influence the morphogenesis of a number of organ systems (3, 4), including the embryonic kidney (25, 27, 28). The PGs, thus, are regarded as critical morphogens, which apparently regulate mammalian embryogenesis under the influence of certain developmentally regulated protooncogenes and growth factors and their receptors (26–32). Conceivably, the decreased expression of PGs may lead to development of congenital defects involving vari-

Address correspondence to Yashpal S. Kanwar, Department of Pathology, Northwestern University Medical School, 303 E. Chicago Avenue, Chicago, Illinois 60611. Phone: 312-503-0084; FAX: 312-503-0627.

Received for publication 30 July 1996 and accepted in revised form 18 September 1996.

J. Clin. Invest.

© The American Society for Clinical Investigation, Inc.

0021-9738/96/12/2478/11 \$2.00

Volume 98, Number 11, December 1996, 2478–2488

1. *Abbreviations used in this paper:* AP-2, activated protein-2; AS, antisense; bFGF-R, basic fibroblast growth factor-receptor; dsODN, double-stranded oligodeoxynucleotide; ECM, extracellular matrix; HS-PG, heparan sulfate proteoglycans; LM, light microscopy; PDN, polydeoxynucleotide; PG, proteoglycan; ROS, reactive oxygen species; RT-PCR, reverse transcriptase-PCR; SE, sense; TdT, terminal deoxynucleotidyl transferase; TUNEL, TdT-mediated dUTP nickend labeling.

ous organs. Since hyperglycemia has been shown to induce alterations in the ECM macromolecules (33–37), it is quite possible that the elevated concentration of glucose would exert dysmorphogenetic effects by adversely affecting the expression of PGs and possibly certain other processes relevant to the embryonic development. In this study, the effect of D-glucose on the metanephric development and the mechanism(s) related to the altered expression of PGs and morphogenesis of the embryonic kidneys were investigated.

Methods

An in vitro culture system was employed to study the effects of elevated concentrations of glucose on organogenesis of murine embryonic kidneys, and metanephrogenesis was evaluated by various morphological and biochemical techniques.

Organ culture system and experimental design. Embryonic kidneys were harvested from fetuses of ICR female mice (Harlan Sprague-Dawley, Inc., Indianapolis, IN) at day 13 of gestation, and maintained in an organ culture system as previously described (27, 28). The initiation point of the culture was designated as day 0, and the kidneys were maintained for 7 d in a serum- and insulin-free culture medium at 37°C in a humidified incubator with a mixture of 95% air and 5% CO₂. The medium consisted of equal volumes of Dulbecco's modified Eagle's medium and Ham's nutrient mixture F12 (Sigma Chemical Co., St. Louis, MO), supplemented with transferrin (50 µg/ml), penicillin (100 µg/ml), and streptomycin (100 µg/ml); pH was maintained at 7.4. Initially, the fetal kidneys were exposed to varying concentrations of D-glucose (5–50 mM), and examined on days 1 to 7 of culture. 30 mM of D-glucose was used for subsequent experiments since, at that concentration, optimal effects with no discernible cytotoxicity were observed by light microscopy (LM) and electron microscopy (EM). L-glucose was used as a control, and ~ 50 explants were used for each time point and variable in various morphological and biochemical studies. The metanephric explants were also radiolabeled with either [³H]thymidine, [³⁵S]methionine, or [³⁵S]sulfate for determining cell replication, de novo synthesis of total and specific ECM proteins, and sulfated proteoglycans under the influence of elevated concentrations of glucose.

Morphological studies. The metanephric explants, from days 1 to 7 of culture were immersion fixed in Karnovsky's paraformaldehyde-glutaraldehyde fixative and processed for LM and EM (27, 28). For LM, serial 0.5-µm-thick sections (~ 100 sections/explant) of EPON-embedded whole metanephric kidneys were prepared and stained with 1% toluidine blue. The coronal sections across the midplane of metanephric explants, which included the maximum number of ureteric bud iterations, were evaluated. For EM, 600-Å-thick sections, which included epithelial as well as mesenchymal components of the metanephric tissues, were examined.

The studies were extended to determine the extent of apoptosis at various stages of metanephric culture under the influence of glucose. An in situ Cell Death Detection Kit (Boehringer Mannheim Biochemicals, Indianapolis, IN) was employed, in which nicked or blunt ends of the DNA strands or the 3'OH ends of the genomic DNA are labeled with fluorescein dUTP and the reaction is catalyzed by terminal deoxynucleotidyl transferase (TdT). This procedure is also known as the TUNEL (TdT-mediated X-d-dUTP nickend labeling) method. For these studies, the explants were immersion fixed in 4% phosphate-buffered (pH 7.4) paraformaldehyde solution for 2 h at 24°C and embedded in paraffin blocks. 4-µm-thick sections were prepared, mounted on clean glass slides, deparaffinized, and rehydrated by treatment with decreasing concentrations of ethanols. After which, the sections were incubated with proteinase K (20 µg/ml in 10 mM Tris-HCl, pH 7.4) for 20 min at 37°C. The sections were then washed with PBS and processed for TUNEL reaction per instructions provided by the manufacturer, and examined with an ultraviolet micro-

scope equipped with epi-illumination. Appropriate positive (DNase-digested) and negative (TdT-untreated) controls were performed during the TUNEL reaction.

[³H]Thymidine incorporation studies. The metanephric explants, exposed to D- or L-glucose for 3 d, were radiolabeled with [³H]thymidine (0.025 mCi/ml) for 12 h, and processed for determination of total incorporated radioactivity and LM autoradiography (27, 28). Mid-point of the culture (day 3) was selected for these experiments since no apparent morphologic changes (i.e., size of the kidney or population of nephrons) were observed in the metanephric explants up to that point. For determination of total incorporated radioactivity, the explants were washed twice with cold medium and treated with 5% trichloroacetic acid for 30 min at 90°C. The hydrolysate was cooled and microfuged, and the supernatant was saved. The DNA content was measured by the diphenylamine method (38), and the total [³H]thymidine incorporation was expressed as disintegrations per minute/microgram DNA. For tissue autoradiographic studies, 0.5-µm-thick sections were mounted onto the glass slides and coated with ILFORD K5 photographic emulsion (Polysciences Inc., Warrington, PA). The sections were developed after 2–3 wk of exposure, photographed, and examined.

[³⁵S]Methionine incorporation and immunoprecipitation studies. Immunoprecipitation studies were performed to evaluate the status of major ECM morphogenetic elements; i.e., type-IV collagen, laminin, and heparan sulfate proteoglycans (HS-PG). The kidneys were treated with D- or L-glucose for 3 d, and then radiolabeled with [³⁵S]methionine (0.25 mCi/ml) for 12 h, and processed for immunoprecipitation as previously described (30–32). After determining the total incorporated radioactivity for each variable, an equal amount of incorporated radioactivity was used for immunoprecipitation with various polyclonal antibodies. The primary antibodies included anti-type IV collagen, -laminin (Gibco Laboratories, Grand Island, NY) and -core protein of HS-PG (30–32). After a second immunoprecipitation with protein-A Sepharose (Pharmacia LKB Biotechnology Inc., Piscataway, NJ), the whole immunoprecipitated product was subjected to SDS-PAGE; the gels were then dried and autoradiograms prepared.

Gene expression studies. Reverse transcriptase-PCR (RT-PCR) technique was employed to study the gene expression of known morphogenetic ECM proteins in metanephric tissues treated with glucose. First, a competitive minigene plasmid DNA construct containing sequences of various ECM proteins and their receptors was synthesized using various primers. The nucleotide sequences of 5' sense (SE) and 3' antisense (AS) primers were derived from data available in Genbank/EMBL/DBJ. The respective sequences of 5'SE and 3'AS primers were as follows: type-IV collagen, 5'-GGGAGCATGAAGGGACAG-3' (5'SE) and 5'-CAGGGCCTTGCTGGCTTC-3' (3'AS); laminin-A chain, 5'-CATGGAAATGCAAGCCAACC-3' (5'SE) and 5'-GCCATGGTGGAGAAGACGCTC-3' (3'AS); perlecan (basement membrane HS-PG), 5'-GCTGTA-GCGGTGACGCATG-3' (5'SE) and 5'-GTTCCGACGCCTGGG-CACAG-3' (3'AS); and β-actin, 5'-GACGACATGGAGAAGATCTGG-3' (5'SE) and 5'-ATGGCCACTGCCGCATCCTC-3' (3'AS). Using these primers and murine embryonic renal cDNA, the PCR products of the expected size of 392 bp (type-IV collagen), 747 bp (laminin A chain), 520 bp (perlecan), and 460 bp (β-actin) were generated, and their authenticity was confirmed by nucleotide sequence analyses, as previously described (30). After determining the suitability of these primers for PCR reactions, two sets of long 5' and 3' polydeoxynucleotide (PDN) single-stranded DNAs in SE and AS orientations with overlapping extensions were synthesized in Northwestern University's biotechnology facility. The 5'SE-PDN (110 mer) included, in seriatum, the nucleotide sequences of type-IV collagen, laminin A chain, perlecan, integrin-α₃, -α₅, and -α₆; while the 5'AS-PDN (105 mer) had sequences of β-actin, fibronectin, basic fibroblast growth factor-receptor (bFGF-R), integrin-α₆, -α₅, and α₃. The 3'SE-PDN (112 mer) included the sequences of type-IV collagen, laminin A chain, perlecan, integrin-α₃, -α₅, and -α₆; while the 3'AS-PDN (109 mer) had sequences of β-actin, fibronectin, bFGF-R, integrin-α₆, -α₅,

and α_3 . The 5' SE- and 5' AS-PDNs were annealed and amplified by PCR to generate a double-stranded DNA with 183-bp product. Similarly, 3' SE- and 3' AS-PDNs were annealed and amplified by PCR to generate a double-stranded DNA with 183-bp product. The 5' and 3' generated products were subjected to blunt end ligation, followed by amplification with PCR, using type-IV collagen 5' sense primer and β -actin 3' antisense primer, to generate a final template DNA with 386 bp; the latter was ligated into pCRTMII cloning vector (Invitrogen Corp., San Diego, CA), and its nucleotide sequence was confirmed by dideoxy chain termination method (30, 31, 39). This template DNA was designated as competitive plasmid DNA to be used in gene expression studies of various ECM proteins. Using the competitive plasmid DNA as a template for primers of various ECM proteins, the expected size of their products is relatively small (221–224 bp), and thus can be easily distinguished from the PCR products generated from murine renal embryonic cDNA.

Renal cDNAs were prepared from metanephric explants exposed to D- or L-glucose for 3 d, as previously described (30–32). Briefly, total RNA was extracted from the metanephric explants by acid guanidinium isothiocyanate-phenol-chloroform extraction method (40). Extracted RNA was digested with RNase-free DNase (1 U/ μ l) in the presence of ribonuclease inhibitor (1 U/ μ l) for 1 h at 37°C. After another chloroform-phenol extraction, the RNA was reprecipitated with ethanol in the presence of RNase-free glycogen (0.1 μ g/ μ l). About 50 μ g of total RNA was used for first strand synthesis using mouse Maloney leukemia virus reverse transcriptase (25 U/ μ l) and oligo (*dt*) as a primer. The cDNA was ethanol precipitated, dried, and resuspended in 50 μ l of deionized autoclaved water and used for competitive PCR analyses. First, linearity relationship between the cDNA and competitive plasmid DNA were determined for each of the ECM proteins. A fixed amount (1 μ l) of "cDNA" from control untreated explants was coamplified with serial logarithmic dilutions (10^{-1} – 10^{-8}) of "competitive minigene plasmid DNA" using sense and antisense primers for a given ECM protein. The reaction mixture included 5 μ l of $10 \times$ PCR buffer (100 mM Tris-HCl, pH 8.3, 15 mM MgCl₂, 500 mM KCl, 0.01% gelatin), 250 μ M of each dNTPs, 1 μ M of 5' sense and 3' antisense primers, and 1 U Taq polymerase (Perkin-Elmer Corp., Norwalk, CT) in a total volume of 50 μ l. The amplification reaction was carried out for a total of 25 cycles in a Thermal Cycler (Perkin-Elmer Corp.) as follows: denaturation at 94°C for 1 min, annealing at 60°C for 1 min, and extension at 72°C for 2 min. The PCR products of cDNA and competitive plasmid DNA were digested with EcoRI, subjected to 2% agarose gel electrophoresis, and photographed using an instant positive/negative film (665; Polaroid Corp., Cambridge, MA). The negatives were analyzed by a scanning densitometer (Hofer Scientific Instruments, San Francisco, CA), and the relative area underneath the tracings was computed. The ratios between the densitometric readings of cDNA- and competitive plasmid DNA-PCR products were plotted using logarithmic scale on the ordinate (y-axis) against the logarithmic dilutions of the competitive plasmid DNA on the abscissa (x-axis). After establishing linearity relationship for the working range, cDNAs isolated from D- and L-glucose-treated explants were subjected to competitive PCR analyses, using primers for type-IV collagen, laminin-A chain, and perlecan. A control analysis was carried out using primers for β -actin.

DNA: protein binding and gel mobility assays. These assays were performed to explore the possible mechanism(s) responsible for the glucose-induced altered expression of one of the major morphogenetic ECM elements, i.e., proteoglycans. The status of activated protein-2 (AP-2) was studied since two viral enhancer AP-2 motifs and three short palindromic direct and indirect repeats have been localized upstream apart from the promoter region of the perlecan, the basement membrane proteoglycan (41). First the nuclear extracts were prepared by following the method described by Dignam et al. (42). Briefly, metanephric explants were transferred to ice cold extraction buffer containing 10 mM Hepes, 1.5 mM MgCl₂, 10 mM KCl, 0.5 mM DTT, and 1 mM PMSF, pH 7.4, and lysed by briefly homogenizing in a Dounce homogenizer. The nuclei were pelleted by centri-

fuging the homogenate at 3,300 g for 15 min at 4°C. The nuclear pellet was suspended in half packed nuclear volume (pnv) of low salt extraction buffer containing 20 mM Hepes, 25% glycerol (vol/vol), 1.5 mM MgCl₂, 20 mM KCl, 0.2 mM EDTA, 0.5 mM DTT, and 0.5 mM PMSF. While stirring the suspended pellet, another half pnv of the same buffer was added, and the KCl concentration was raised to 1.2 M. The stirring was continued for 30 min at 4°C, following which the extract was centrifuged at 25,000 g for 30 min. The supernatant was saved and dialyzed against two changes of 50 vol buffer containing 20 mM Hepes, 20% glycerol (vol/vol), 0.1 M KCl, 0.2 mM EDTA, 0.5 mM DTT, and 1.0 mM PMSF for 6 h. Aliquots of each variable were made after adjusting the final protein concentration to 1 μ g/ μ l, and stored at -80°C until further use.

A double-stranded oligodeoxynucleotide (dsODN) with AP-2-specific recognition sequences (i.e., 5'-GAACTGACCGCCCGCGGCCG TG-3') (43) was synthesized and radiolabeled with [$\gamma^{35}\text{S}$]-ATP using T4 polynucleotide kinase. The binding reaction mixture included 1:10 diluted Hepes buffer (Hepes 10 mM, pH 7.9, 1.2 M NaCl, 10 mM MgCl₂, 10 mM DTT, and 1 mM EDTA), dsODN (10,000 cpm), 5 μ g poly [d(I-C)], 10 μ g nuclear protein extract, and BSA with a final concentration of 300 μ g/ml. The reaction was carried out at 30°C for 15 min. Specificity of the binding was ascertained by adding either 10 times excess unlabeled dsODN to competitively inhibit DNA-protein interactions or anti-AP-2 antibody (Upstate Biotechnology Inc., Lake Placid, NY) in various reaction mixtures. Additional experiments were carried out in which explants were concomitantly exposed to glucose and insulin (0.6 U/ml). The binding complexes from all the reactions were subjected to native (nondenatured) 5% polyacrylamide gel electrophoresis at 4°C. The gels were dried, and autoradiograms prepared.

Experiments with ATP. Another mechanism by which glucose could induce altered perlecan expression may relate to the depletion of energy stores, as observed with other aldohexoses (34). Thus, intracellular levels of ATP were determined by hexokinase reaction method described by Lang and Michael (44) in glucose-treated metanephric explants. They were exposed to D- or L-glucose for 1–9 h in the presence or absence of [^{35}S]sulfate (0.5 mCi/ml); the latter was used to radiolabel the sulfated proteoglycans. Thereafter, the explants were immediately homogenized in ice cold 0.3 M perchloric acid. After an equilibration on ice for 10 min, the homogenate was centrifuged at 5,000 g for 15 min at 4°C, and supernatant was neutralized to pH 7.0. 100- μ l aliquots were prepared and stored at -70°C . 1 ml of reagent mixture (50 μ M Tris, pH 8.0, 100 mM glucose, 0.1 mM MgCl₂, 50 μ M NADP⁺, and 0.08 μ g/ml glucose-6-phosphate) was added to each thawed aliquot. Fluorometer readings were recorded before and 10 min after the addition of 10 μ l hexokinase (0.1 μ g/ml) to the reaction mixture. The ATP concentration was calculated by comparing the values to a standard curve, and ultimately expressed as nanomoles of ATP per metanephric explant. For the repletion experiments, 100 μ M ATP was included in the medium in the presence or absence of D- or L-glucose. In these experiments, the media containing fresh ATP was changed every 4 h for the entire culture period up to 7 d. The explants radiolabeled with [^{35}S]sulfate were extracted with 4 M guanidine-HCl solution containing a mixture of protease inhibitors (27). The extracts were subjected to DEAE-Sephacel chromatography (Pharmacia LKB Biotechnology Inc.) using a continuous gradient of 0.1–1.0 M NaCl in 8 M urea solution containing 50 mM sodium acetate and 0.2% 3-[(3-cholamidopropyl)-dimethylammonio]-1-propanesulfonate (CHAPS, Sigma Chemical Co.), pH 6.0 (32). The incorporated radioactivity in fractions eluted above 0.3 M NaCl concentration was determined and normalized to per microgram of protein.

Results

Normally, in vivo, the kidney develops by reciprocal inductive interaction of the ureteric epithelial bud with the undifferentiated metanephric mesenchyme (24). As a result, nephron de-

velopment ensues with differentiation of induced mesenchyme into epithelial phenotype, which undergoes a series of developmental stages; i.e., vesicle, comma, and S-shaped body stages. The distal portion of the S-shaped body differentiates into a precapillary stage glomerulus, while its proximal antipolar segment develops into proximal and distal tubules. These stages are also seen in developing metanephroi maintained for

1–10 d in an in vitro serum-free organ culture system. Being a serum-free culture system, the effects of various modulators of renal growth can be readily studied. This investigation relates to the study of glucose-induced alterations in the developing metanephros and the elucidation of mechanism(s) responsible for its dysmorphogenesis.

D-Glucose-induced morphological characteristics. Metanephroi were examined 1, 4, and 7 d after exposure of glucose. By light microscopy, no appreciable changes in the morphology were observed after day 1. By day 4, a mild decrease ($\sim 10\%$) in the size of the metanephroi and nephron population was noted. The alterations were mainly observed on the 7th day of exposure to D-glucose. They included reduction ($\sim 50\%$) in the size of metanephroi and population of nephron elements (Fig. 1, B vs. A). Very few well-developed nephrons (i.e., precapillary-stage glomeruli) and tubules were observed (Fig. 1 B). Vesicle and S-shaped body elements were not present. Notably, the metanephric mesenchyme was atrophic and included cells with condensed nuclei (Fig. 1 B, *small arrows*). The ureteric bud and its primary iterations were thickened, while the secondary iterations of the ureteric bud were rudimentary and exhibited a marked degree of branching dysmorphogenesis and atrophy. The tertiary iterations were absent. The tips of the ureteric bud branches, the site of nascent nephron formation, were blunted and had lost their acuteness. The control metanephroi exposed to L-glucose did not reveal any signifi-

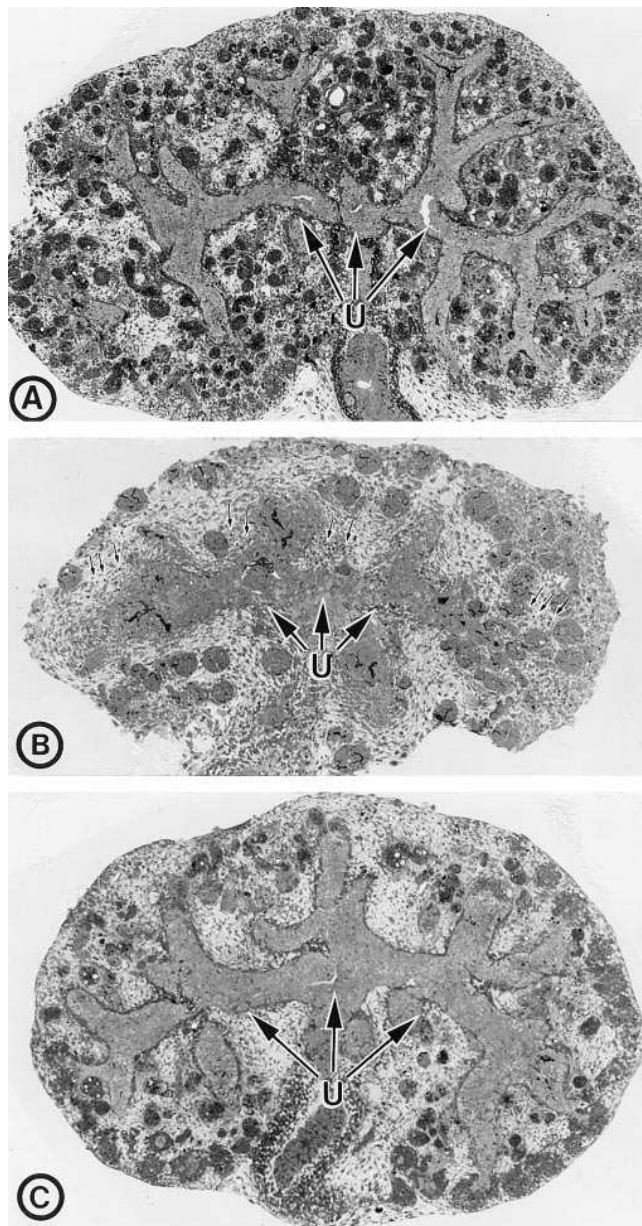


Figure 1. Light micrographs of the metanephric explants exposed for 7 d to L-glucose (A), D-glucose (B), and D-glucose + ATP (C). The D-glucose-treated embryonic kidney is smaller and has fewer nephrons, and it exhibits branching dysmorphogenesis of the ureteric bud (U) and atrophy of the mesenchyme. The poor arborization and blunting of the tips of ureteric bud branches are suggestive of defective epithelial/mesenchymal interactions. The atrophic mesenchyme has many condensed nuclei, which is reflective of cells undergoing apoptosis (B, *small arrows*). With the addition of ATP (C), a partial restoration of morphological characteristics of the metanephric explant is observed. $\times 30$.

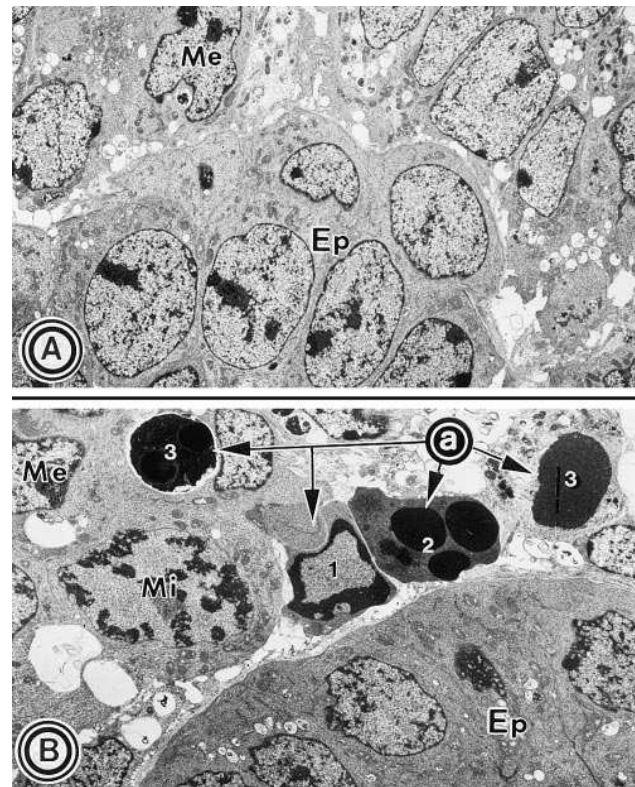


Figure 2. Electron micrographs of (A) L-glucose- and (B) D-glucose-treated metanephric explants showing cellular changes at the mesenchymal (Me)/epithelial (Ep) interface. In D-glucose-treated embryonic kidney, many mesenchymal cells (Me) in various stages of apoptosis (a, 1–3) are seen. A few mitotic figures (Mi) are also seen. The epithelial cells (Ep) are relatively unaffected. $\times 2,500$.

cant pathologic changes, and normal branching morphogenesis of the ureteric bud branches and nephron development was seen (Fig. 1 A). Ultrastructural examination of metanephroi treated with D-glucose for 7 d revealed changes, which were mostly confined to the mesenchymal cells. The changes included the apoptosis of the mesenchymal cells in the vicinity of the epithelial phenotype of the ureteric bud branches or nephron elements. In some fields, the apoptotic bodies in different stages of development were observed (Fig. 2 B). Many cellular nuclei had peripheral crescents of compacted chromatin (Fig. 2 B, I), while others had condensed chromatin bodies (Fig. 2 B, 2). In some cells, the whole nuclear chromatin was uniformly condensed (Fig. 2 B, 3). A few mesenchymal cells undergoing mitosis were also seen adjacent to the apoptotic bodies. The embryonic kidneys exposed to L-glucose did not reveal any significant ultrastructural alterations (Fig. 2 A). The extent of apoptosis, which is usually best assessed by electron microscopy (vide supra), was further evaluated by the TUNEL procedure that employs labeling of apoptotic cells with fluoresceinated dUTP. The metanephroi exposed to D-glucose for 1 d showed minimal differences in the labeling of cells as compared with the control L-glucose (Fig. 3 B vs. A). At day 4 of the organ culture, a mild increase in the labeling of the cells was observed in explants treated with D-glucose (Fig. 3 D vs. C). Notable differences were observed on day 7, where a remarkable increase in the labeling of apoptotic cells was ob-

served in D-glucose-treated metanephroi compared with the control (Fig. 3, F vs. E). Interestingly, most of the labeled apoptotic cells were confined to the metanephric mesenchyme, and a few in the ureteric bud.

[³H]Thymidine incorporation studies. These studies were performed on day 3 of the culture, the time antedating any discernible morphological changes, as observed by light and electron microscopy and by the TUNEL method. The total [³H]thymidine-associated incorporated radioactivity in the whole explants was decreased in D-glucose-treated kidneys as compared with the control (32.04 ± 2.25 vs. 41.35 ± 3.18 dpm/ μ g DNA, $n = 50$). Tissue autoradiography of the explants labeled with [³H]thymidine also showed a moderate reduction in the incorporated radioactivity, as reflected by the reduced number of silver grains (Fig. 4, B vs. A). The reduction of silver grains was mainly confined to the outer cortex or nephrogenic zone of the metanephros, the site where active epithelial/mesenchymal interactions take place. No significant differences were observed in the remaining parenchyma of the metanephros, suggesting that, like apoptosis, the major changes are confined to the metanephric mesenchyme, the latter being programmed to differentiate into epithelial phenotype, and where maximal cell replication occurs.

Status of various extracellular matrix components. Since the reciprocal epithelial/mesenchymal interactions are influenced by the ECM, the studies to assess the glucose-induced alter-

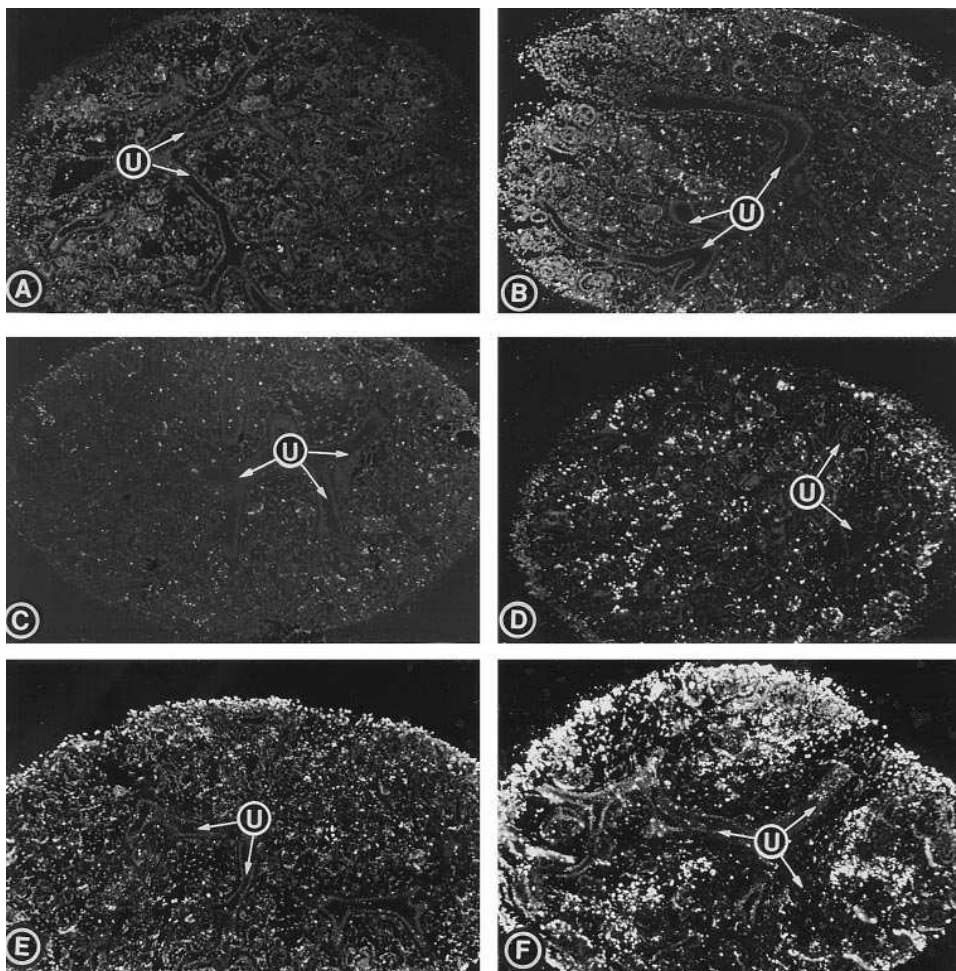


Figure 3. Fluorescence micrographs showing dUTP-labeled apoptotic cells of the metanephric explants treated with L-glucose (A, C, and E) and D-glucose (B, D, and F) for 1 (A and B), 4 (C and D) and 7 d (E and F). The sections of the explants were incubated with fluorescein-labeled dUTP, and the reaction was catalyzed by TdT. The explants treated with D-glucose for 7 d show nuclei of numerous mesenchymal cells labeled with fluoresceinated dUTP (F), indicating a marked degree of apoptosis. Ureteric bud branches (U) show minimal labeling of the cells. The control explants treated with L-glucose exhibit a remarkably lesser degree of labeling of cells with dUTP (A, C, and E). $\times 25$.

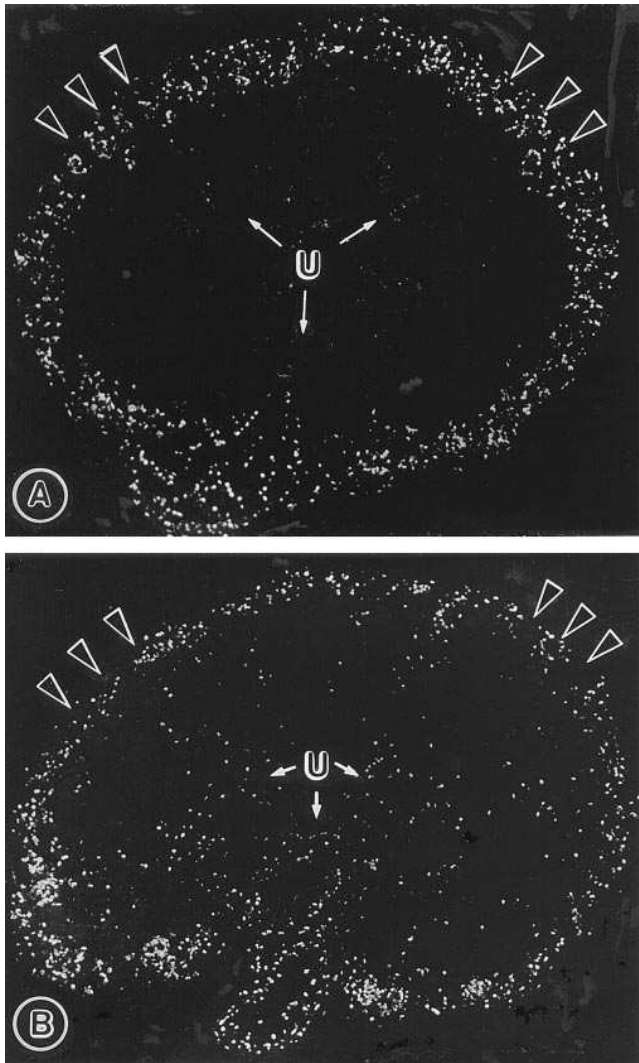


Figure 4. Dark field microscopic autoradiograms of (A) L-glucose- (B) D-glucose-treated metanephric explants for 3 d in culture, and then labeled with [³H]thymidine. In control (A), the nephrogenic zone (arrowheads) of the explant is heavily labeled with [³H]thymidine. The explants treated with D-glucose (B) show remarkably less radioactivity in the nephrogenic zone. The ureteric bud branches (U) show minimal labeling. $\times 30$.

ations in the de novo synthesis of proteins by the metanephroi were performed. Initially, the effect on overall protein synthesis was determined in metanephroi exposed to glucose for 3 d in culture. A mild reduction in [³⁵S]methionine-associated incorporated radioactivity was observed in D-glucose-treated kidneys as compared with the control ($3.72 \pm 0.25 \times 10^7$ vs. $4.65 \pm 0.32 \times 10^7$ dpm/explant, $n = 50$). Although the D-glucose induced only a mild decrease in total incorporated radioactivity, the immunoprecipitation experiments revealed notable changes in the ECM components, especially in the expression of HS-PG. A marked decrease (\sim fourfold) in the anti-HS-PG immunoprecipitated incorporated radioactivity was observed in explants treated with D-glucose as compared with L-glucose (Fig. 5). Also, the autoradiograms of agarose-PAGE revealed remarkably reduced intensity of the HS-PG band (Fig. 5, left). Similarly, anti-HS-PG immunoprecipitated [³⁵S]sulfate-asso-

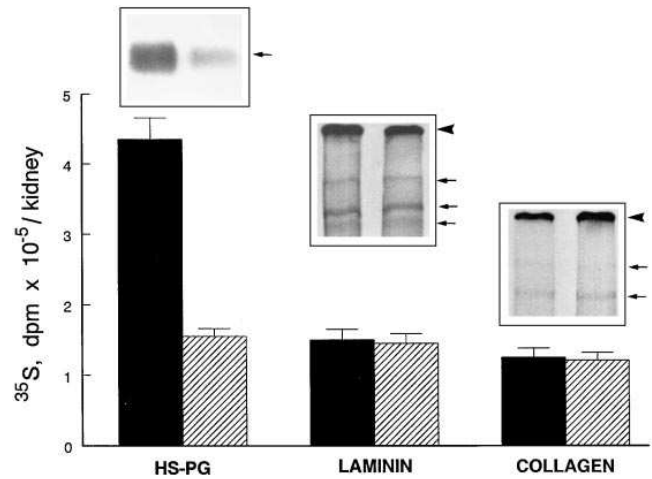


Figure 5. SDS-PAGE autoradiograms of the immunoprecipitated radioactivity with anti-HS-PG, laminin, and type-IV collagen antibodies. The explants were exposed to L- and D-glucose for 3 d, labeled with [³⁵S]methionine, and an equal amount of incorporated radioactivity was used for immunoprecipitation. A marked decrease in the radioactivity associated with the HS-PG fraction is observed. Minimal decrease in the radioactivities associated with laminin and type-IV collagen is observed. Arrows indicate migration of the bands, and arrowheads indicate point of application of the samples. ■, L-glucose; ▨, D-glucose.

ciated radioactivity, reflective of sulfated proteoglycan synthesis, was decreased in explants treated with D-glucose ($1.21 \pm 0.15 \times 10^5$ vs. $3.63 \pm 0.32 \times 10^5$ dpm/explant, $n = 50$; see Fig. 12). The autoradiograms of SDS-PAGE of laminin and type-IV collagen revealed no significant decrease in the intensity of the bands, suggesting minimal alterations in the de novo synthesis of their chains (Fig. 5, middle and right). Also, a minimal decrease in the incorporated radioactivity associated with laminin and type-IV collagen was observed.

Gene expression studies. Since immunoprecipitation studies suggested altered expression of certain ECM components,

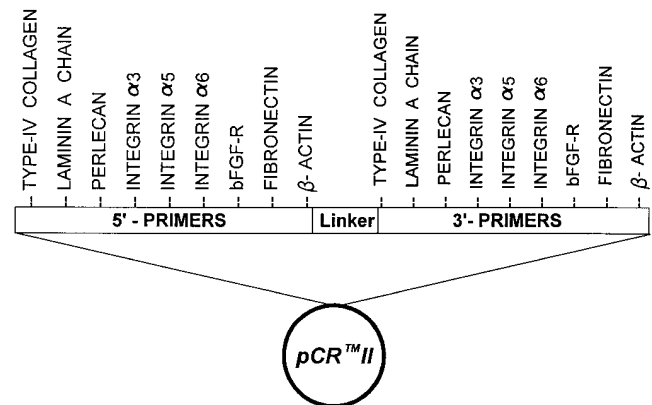


Figure 6. Schematic drawing of the minigene construct, which was ligated into pCRTMII plasmid. It includes primers with nucleotide sequences specific for various matrix proteins and their receptors, and it was used as a competitive DNA template for RT-PCR analyses. The nucleotide sequence is available under Genbank/EMBL/DBJ accession No. U17140.

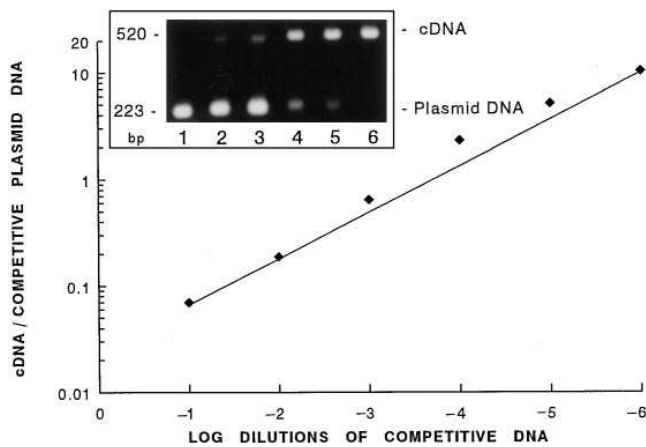


Figure 7. Competitive RT-PCR of perlecan (HS-PG) cDNA prepared from embryonic kidneys, harvested at day 13 of gestation. A fixed amount of first strand cDNA and logarithmic dilutions of competitive plasmid DNA were used as templates for the amplification of the PCR products. The amplified products exhibit linearity between the logarithmic dilutions (10^{-1} to 10^{-6} , lanes 1–6) of competitive DNA and the ratio of amplified perlecan cDNA (upper bands) to plasmid DNA (lower bands).

studies to ascertain whether or not the D-glucose-induced changes are also related to the alterations in the posttranscriptional events were performed. Because a large number of explants (i.e., 500–1,000 per variable) are needed for Northern blot analysis, RT-PCR was employed to assess the gene expression. First a minigene construct, to be used for competitive RT-PCR analyses, was prepared (Fig. 6). Its nucleotide sequence (Genbank/EMBL/DBJ accession No. U17140), including the position of various primers for ECM components and related receptor molecules, is as follows:

```

5'...GGGAGCATGAAGGGACAG...CATGGAATGCAAGCCAACC...GCTGCTAGCGGTGACGCATG...
   type-IV collagen      laminin A chain      perlecan
...CCTCCAGACACCTCCAACA...CCAAGTGTTCAGGCTGCGC...GACTCTTAAGTGTAGCGTGA...
   α3 integrin          α3 integrin          α4 integrin
...GAATGTCTCCTTGAGGATG...CCCCGCCCTGGTGCACGGAGGCC...GACGACATGGAGAAGATCTGG...
   bFGF-R              fibronectin          β-actin
...GAATTCCTCCCTCTGCAG...
   linker
...CAGGGCCTGTGGCTTC...GCCATGGTGGAGAAGACGCTC...GTTCCGACGCTGGGCACAG...
   type-IV collagen      laminin A chain      perlecan
...GCTACCCACCAAGAAGCACTG...GGAAAAAGCTCAGCTCAAG...CGGAAAGAAGAGGAGAGAT...
   α3 integrin          α3 integrin          α4 integrin
...GCCACGAGACAGACTGGTCT...GGCACTGACGAAGAGCCCTTACAG...ATGGCCACTGGCCATCTC...3'
   bFGF-R              fibronectin          β-actin

```

Using this construct and the cDNA prepared from explants harvested at day 13 of gestation, a linearity in the ratios of PCR products of perlecan cDNA to minigene plasmid DNA could be maintained when plotted against 10^{-6} serial logarithmic dilutions of competitive plasmid DNA (Fig. 7). Within this range of serial dilutions, the bands of embryonic kidney cDNA and plasmid DNA PCR products of perlecan were discernible for densitometric analyses to obtain a ratio, and thus we proceeded to RT-PCR analyses on explants treated with glucose for 3 d. In control (L-glucose) explants, the ratio in the intensity of the bands maintained a linearity up to a dilution of 10^{-4} , while in D-glucose-treated explants, the competitive plasmid DNA needed to be diluted further, (i.e., to 10^{-8}) to visualize the bands and obtain a ratio (Fig. 8). This suggests a marked decrease in the concentration of perlecan cDNA, reflective of mRNA expression, under the influence of D-glucose. Similarly, after establishing the linearity relationships for other extracellular matrix proteins, RT-PCR analyses were performed for the expression of type-IV collagen and laminin. In contrast to the remarkable decrease in perlecan, the mRNA expressions for type-IV collagen and laminin A chain were minimally affected by the D-glucose treatment (Fig. 9). No significant differences in the β -actin expression were observed between the D- and L-glucose-treated kidneys.

DNA: protein binding analyses. Since AP-2 motifs are present in the promoter region of the perlecan, their functionality was assessed in these studies, which could explain the reduced

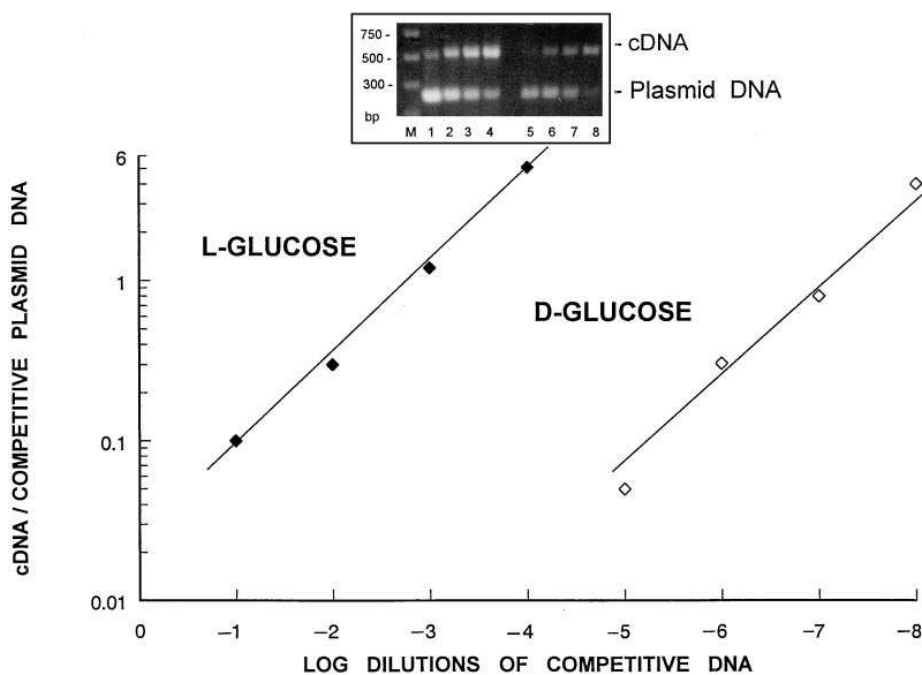


Figure 8. Competitive RT-PCR of perlecan (HS-PG) cDNAs, prepared from embryonic explants treated with L- (lanes 1–4) and D-glucose (lanes 5–8) for 3 d. Serial logarithmic dilutions of competitive plasmid DNA and a fixed amount ($1 \mu\text{l}$) of first strand perlecan cDNA were coamplified. The ratios between the densitometric readings of cDNA and competitive plasmid DNA PCR products were plotted on logarithmic scales on the ordinate (y-axis) against the logarithmic dilutions of competitive DNA on the abscissa (x-axis). A relative reduction in the amplification of cDNA, isolated from embryonic kidneys treated with D-glucose, is observed compared with the control; i.e., L-glucose-treated explants. The lane M represents the molecular weight markers.

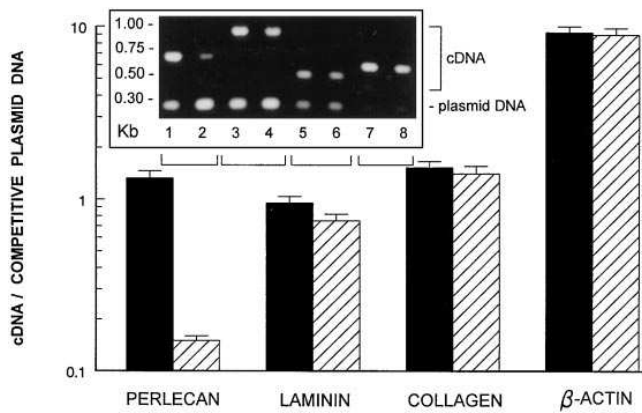


Figure 9. Gene expression of various ECM proteins, analyzed by quantitative RT-PCR. Lanes 1, 3, 5, and 7 represent amplified PCR products of cDNAs prepared from L-glucose-treated explants. Lanes 2, 4, 6, and 8 represent PCR products of cDNAs prepared from D-glucose-treated kidneys. A notable reduction in the HS-PG/perlecan (lanes 1 and 2) gene expression is observed in metanephric explants treated with D-glucose. Minimal differences in the gene expressions of laminin (lanes 3 and 4), type-IV collagen (lanes 5 and 6), and β -actin (lanes 7 and 8) are observed. ■, L-glucose; ▨, D-glucose.

mRNA expression observed with the exposure of metanephric explants to D-glucose for 3 d. Thus, nuclear extracts, prepared from L- and D-glucose-treated kidneys were incubated with [γ^{35} S]ATP-labeled AP-2 dsODN, followed by nondenaturing polyacrylamide gel electrophoresis and preparation of autora-

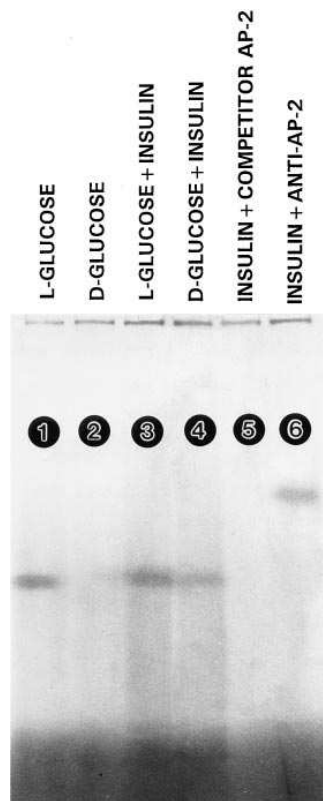


Figure 10. Autoradiogram showing the effect of glucose on the binding activity of transcription factor AP-2. Nuclear extracts were prepared from explants treated with glucose alone and in the presence of insulin. The extracts were incubated with [γ^{35} S]ATP-labeled dsODN containing AP-2 binding sequences. The incubation mixtures were then subjected to polyacrylamide gel electrophoresis. A decrease in the binding activity of AP-2 is observed in the nuclear extracts prepared from the explants treated with D-glucose (lane 2). The DNA/protein interactions were restored by the concomitant treatment of explants with insulin (lane 4). The unlabeled dsODN competitively inhibited the binding of radiolabeled dsODN (lane 5). A shift in the band of radioactivity (arrows) to a higher position after incubation of the dsODN/nuclear extract mixture with the anti-AP-2 antibody (lane 6) established the specificity of the DNA/protein interactions.

diagrams. In the D-glucose-treated group, a notable decrease in the intensity of autoradiographic bands was observed as compared with the control (Fig. 10, lane 2 vs. 1), suggesting possibly a reduced concentration in the active moiety of AP-2 binding protein(s) or alternatively, interference in the DNA/protein interactions. With the addition of insulin in the organ culture medium, the intensity of the autoradiographic band increased. The intensity was higher in explants treated with insulin + L-glucose vs. insulin + D-glucose (Fig. 10, lanes 3 and 4), suggesting an increased phosphorylation of binding proteins or normalization of the DNA/protein interactions. Specificity of DNA/protein interactions was established by competition experiments, in which 10-fold excessive unlabeled AP-2 dsODN was added to the incubation mixture. In this competition experiment, no autoradiographic band was observed (Fig. 10, lane 5). The specificity was further confirmed by gel shift assay, in which specific AP-2 antibody was added to the incubation mixture. With the inclusion of the AP-2 antibody in the incubation mixture, the autoradiographic band shifted to a

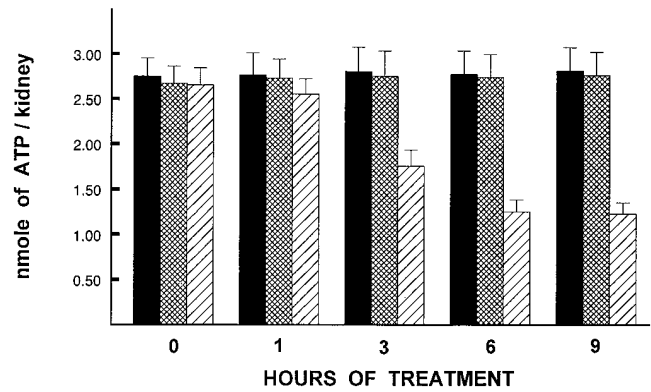


Figure 11. Concentrations of cellular ATP in untreated (control) metanephric explants, and kidneys treated with L- and D-glucose. A 50% drop in the concentration of ATP is observed with the treatment of D-glucose after 9 h. No further drop in the ATP concentration is observed with further extension of the treatment ($n = 50$). ■, control; ▨, L-glucose; ▩, D-glucose.

diagrams. In the D-glucose-treated group, a notable decrease in the intensity of autoradiographic bands was observed as compared with the control (Fig. 10, lane 2 vs. 1), suggesting possibly a reduced concentration in the active moiety of AP-2 binding protein(s) or alternatively, interference in the DNA/protein interactions. With the addition of insulin in the organ culture medium, the intensity of the autoradiographic band increased. The intensity was higher in explants treated with insulin + L-glucose vs. insulin + D-glucose (Fig. 10, lanes 3 and 4), suggesting an increased phosphorylation of binding proteins or normalization of the DNA/protein interactions. Specificity of DNA/protein interactions was established by competition experiments, in which 10-fold excessive unlabeled AP-2 dsODN was added to the incubation mixture. In this competition experiment, no autoradiographic band was observed (Fig. 10, lane 5). The specificity was further confirmed by gel shift assay, in which specific AP-2 antibody was added to the incubation mixture. With the inclusion of the AP-2 antibody in the incubation mixture, the autoradiographic band shifted to a

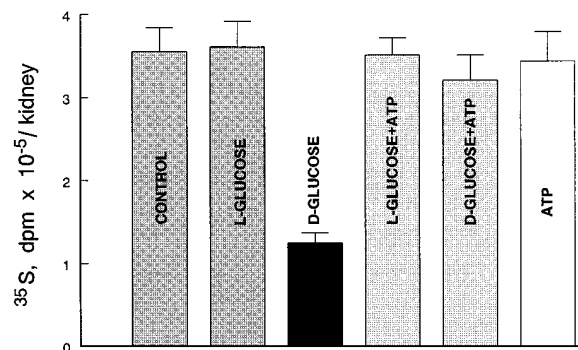


Figure 12. [35 S]Sulfate incorporated radioactivity per metanephric kidney in the absence (control) and presence of L-glucose, D-glucose, L-glucose + ATP, D-glucose + ATP, and ATP alone. A notable decrease in the [35 S]sulfate incorporation was observed in the explants exposed to D-glucose, and addition of ATP restored the radioincorporation ($n = 50$).

higher position (Fig. 10, lane 6). These results suggest that the reduced mRNA expression by D-glucose treatment may be related to perturbed DNA/protein interactions regulating the events confined to upstream of the promoter region of the perlecan gene, which may be due to the activation, either by phosphorylation or by some other modification, of AP-2 binding proteins.

ATP analyses and [³⁵S]sulfate incorporation. Another mechanism that could explain the reduced expression of perlecan mRNA may relate to the decreased intracellular ATP pool, which in turn are likely to affect various phosphorylation events. Thus, ATP concentration was measured in the untreated explants, and those treated with D- or L-glucose for 1 to 9 h. An appreciable reduction in the ATP was observed in explants exposed to D-glucose for 3 h (Fig. 11). The ATP levels decreased progressively with further exposure to D-glucose for 9 h, and remained at this level for the remainder of the culture period. No appreciable decrease in the ATP levels were observed in explants treated with L-glucose. Concomitantly, a reduced [³⁵S]sulfate incorporation, reflective of de novo synthesis of sulfated proteoglycans, was observed (Fig. 12). The incorporated radioactivity associated with proteoglycans is mainly confined to the fractions eluted above 0.3 M NaCl DEAE-Sephacel gradient, as previously described (28, 32). Besides a decrease in the [³⁵S]sulfate incorporation, the major elution peak of the radioactivity in DEAE-Sephacel chromatogram was lower in explants treated with D-glucose as compared with the control (0.38 vs. 0.45 M). These elution-gradient profiles suggested a decrease in the charge-density characteristics of the sulfated PGs synthesized under the influence of D-glucose. The [³⁵S]sulfate incorporation was not significantly affected by the L-glucose treatment. Interestingly, addition of exogenous ATP (100 μM/ml) into the culture medium resulted in a notable improvement in the [³⁵S]sulfate incorporation (Fig. 12). The ATP alone did not increase the [³⁵S]sulfate incorporation from the basal levels in untreated embryonic explants. Lastly, exogenous addition of ATP into the medium also improved the morphological characteristics of the explants cultured in the presence of D-glucose (Fig. 1 C). The explant size was ~ 80% of the control L-glucose-treated embryonic kidneys. Although, a total recovery could not be achieved, the primary, secondary, and tertiary iterations of the ureteric bud branches, although thickened, were readily discernible. The acuteness of the tips of ureteric bud branches was not completely restored; however, the nephron population was much higher as compared to those in D-glucose treated explants (Fig. 1, C vs. B), and a relatively few cells with condensed nuclei were seen in the metanephric mesenchyme.

Discussion

Recent in vitro studies on the rat embryo suggest that some of the aldohexoses, including mannose, fructose, galactose, and glucose, exert teratogenic effects that are mainly confined to the caudal half of the fetus (13, 14, 23), but organ-specific glucose-induced dysmorphogenesis and the relevant mechanism(s) remain to be described. The present study reports D-glucose-induced dysorganogenesis of the embryonic kidneys (Fig. 1). The dysmorphogenesis seems to be specific to D-glucose since L-glucose failed to induce any alterations in the embryonic kidney, suggesting the mechanism(s) involved are unrelated to nonenzymatic glycation (45). In renal devel-

opment, integrity of the mesenchyme and ureteric bud and proper epithelial/mesenchymal interactions are necessary for differentiation of the mesenchymal cells and formation of nephrons (24). Thus, the abnormalities, such as branching dysmorphogenesis of the bud and loss of acute angularity of its tips, are expected to perturb proper epithelial/mesenchymal contacts, and thereby to induce dysmorphogenesis of the kidney. The disruption of epithelial/mesenchymal contacts leading to dysmorphogenesis of the kidney with atrophy of the mesenchyme has been reported in other studies as well (28, 46). The atrophy of the mesenchyme not only leads to the cessation of nephrogenesis, but also to apoptosis of the mesenchymal cells (46).

The apoptosis in the atrophic mesenchyme (Figs. 2 and 3) may partly be related to the perturbed epithelial/mesenchymal interactions, and partly to the direct inhibitory effects on DNA synthesis, since a reduced [³H]thymidine incorporation was observed in the presence of glucose (Fig. 4). Using [³H]thymidine incorporation assay and acridine orange staining, other aldohexoses (e.g., galactose) have been shown to alter cell replication and induce apoptosis in ocular epithelial cells (47). The findings of this investigation indicate that glucose can also affect the embryonic epithelial as well as mesenchymal cells. In vivo, the metanephric mesenchyme undergoes a certain degree of apoptosis during the initial stages of postinductive period of development (i.e., at days 12–14) and it regresses rapidly by the 15–17th day of gestation (48). In the in vitro system, a mild degree of apoptosis was also observed in the controls, while it was drastically accentuated by the D-glucose treatment (Figs. 2 and 3). How the glucose accentuates or induces apoptosis, directly or indirectly, remains to be investigated. Available data indicate that apoptosis ensues with the inhibition of protein kinase C, activation of interleukin-1β converting enzyme-like enzymes, *Caenorhabditis elegans* cell death gene-3-like proteases and of calcium-sensitive endonucleases (49). The apoptosis can be inhibited by growth factors that use receptors with tyrosine kinase catalytic domains (46). More recently, the apoptosis has also been shown to be influenced by reactive oxygen species (ROS) (50, 51). Since ROS scavengers exert a protective effect against the aldohexose-induced embryonic malformations in vitro (21), one may speculate that glucose treatment generates ROS that result in the apoptosis of the mesenchyme and subsequent renal dysmorphogenesis.

Besides apoptosis, the glucose-induced dysmorphogenesis may also be related to the alterations in the expression of morphogenetic ECM proteins, including PGs, laminin, fibronectin, and type-IV collagen. Previous observations indicate considerable alterations in the expression of type-IV collagen, laminin, and fibronectin, and in the matrix receptors in hyperglycemic state or in the presence of elevated concentrations of glucose in the medium (16, 33, 35, 36, 52–55); however, in embryonic tissues, their expression seems to be largely unaffected (Figs. 5–9). The variations in these findings may be related to the culture conditions used where the cells have undergone certain phenotypic drifts; in the case of in vivo systems, one may be dealing with the prolonged effect of hyperglycemia in the presence of circulating cytokines; e.g., growth factors. Alternatively, the effects may not be readily discernible in the organ culture of a relatively short duration since the turnover of some of these ECM proteins (e.g., laminin) is rather low (34). The decreased expression of HS-PG observed in this study is in line with previous observations made in other systems by us

and others (34, 37, 56). The morphogenetic effects of the PGs are probably related to the glycosaminoglycan (GAG) chains attached to the core peptide (57, 58) since the elimination of GAGs leads to dysorganogenesis (27, 28, 59). Thus, the decreased expression of PGs, and consequential deficit of GAGs, led to the dysmorphogenesis of metanephros in the presence of D-glucose.

The question as to how glucose reduces the expression of PGs needs to be addressed. A number of mechanisms may be involved, including the effects mediated by ROS, since they induce structural damage in the PGs (60). Other mechanisms may relate to the alterations in transcription, since both the protein as well as gene expressions of the HS-PG were affected (Figs. 5 and 9). Structural analysis of the 5' end and upstream region of the HS-PG (perlecan) has revealed the presence of two viral enhancer AP-2 motifs and three small palindromic repeats, which by forming secondary structures may regulate the expression of HS-PG (41). AP-2 mediates transcriptional activation either via cAMP-dependent protein kinase A or via phorbolster- and diacylglycerol-activated protein kinase C (43). The protein kinase C is ubiquitously distributed in various tissues and it has been reported to alter the gene expression of certain ECM proteins; e.g., laminin, type-IV collagen, and fibronectin (61). Presumably, protein kinase C-induced fibronectin expression is mediated by the transcription factor AP-1 (53). The role of AP-1 in the expression of other matrix proteins remains to be investigated. In this investigation, studies were concentrated on the activity of AP-2 only since no AP-1 binding motifs are found in the promoter region of the HS-PG gene. With the D-glucose exposure, a marked reduction in the activity of AP-2 was observed (Fig. 10), suggesting that glucose either reduced the intracellular concentration of AP-2 or its active moiety. The latter possibility is likely since insulin could normalize the DNA/protein interactions, conceivably by phosphorylation of the transcription factor AP-2 (Fig. 10).

The above observations indicate that glucose may perturb various metabolic events that are dependent on intracellular phosphorylation or energy stores; i.e., ATP. In this regard, other aldohexoses (e.g., mannose) have been shown to induce depletion of ATP (13, 14, 22, 34). The results of the present investigation indicate that, in addition to mannose, glucose can also induce depletion of cellular ATP (Fig. 11). The decrease in ATP may lead to a reduced phosphorylation of AP-2, and consequential reduced gene expression of PGs. The decreased expression of PGs may also be directly affected by the depletion of ATP stores, since the PGs are heavily glycosylated and require substantial amounts of ATP for their synthesis and posttranslational modifications, including sulfation. A decreased [³⁵S]sulfate incorporation and lower charge-density of the PGs, observed under the influence of D-glucose, would support such a contention (Fig. 12). Further support for this contention is provided by the fact that exogenous addition of ATP into the medium normalized the [³⁵S]sulfate incorporation, proteoglycan expression and metanephric morphology (Figs. 1 and 12). All the above described D-glucose-induced effects may be related to alterations in intracellular phosphorylation; however, the induction of apoptosis, an energy-dependent process (62), remains unexplained. Conceivably, the intracellular ATP stores were sufficient to sustain the events involved in the induction of apoptosis. The fact that an absolute depletion of ATP could not be achieved throughout

the entire period of metanephric culture would be supportive of such a notion. Finally, it is quite apparent from the findings of the present study that D-glucose-induced metanephric dysmorphogenesis is an intriguing phenomenon, and it would certainly require further extensive investigatory efforts to delineate the interdependence of various mechanisms involved at each step relevant to this complex process.

Acknowledgments

This investigation was supported in part by National Institutes of Health grant DK-28492.

References

- Price, R.B., and B.G. Hudson. 1987. Renal Basement Membranes in Health and Disease. Academic Press Inc., New York. 439 pp.
- Striker, G.E., E.P. Peten, M.A. Carome, C.M. Pesce, K. Schmidt, C.W. Yang, S.J. Elliot, and L.J. Striker. 1993. The kidney disease of diabetes mellitus (KDDM): a cell and molecular biology approach. *Diabetes Metab. Rev.* 9:37-56.
- Toole, B.P. 1991. Proteoglycan and hyaluronan in morphogenesis and differentiation. In *Cell Biology of Extracellular Matrix*. E.D. Hay, editor. Plenum Press, New York. 305-342.
- Eklblom, P. 1993. Basement membranes in development. In *Molecular and Cellular Aspects of Basement Membranes*. D.H. Rohrbach, and R. Timpl, editors. Academic Press, Inc., New York. 359-383.
- Pederson, L.M., I. Tygstrup, and J. Pederson. 1964. Congenital malformations in newborn infants of diabetic women: correlations with maternal diabetic vascular complications. *Lancet*. i:1124-1126.
- Comess, L.J., P.H. Bennett, T.A. Burch, and M. Miller. 1969. Congenital anomalies and diabetes in the Pima Indians of Arizona. *Diabetes*. 18:471-477.
- Soler, N.G., C.H. Walsh, and J.M. Malins. 1976. Congenital malformations in infants of diabetic mothers. *Q. J. Med.* 45:303-313.
- Fuhrmann, K., H. Reihar, K. Semmler, F. Fischer, M. Fischer, and E. Glockner. 1983. Prevention of congenital malformations in infants of insulin-dependent diabetic mothers. *Diabetes Care*. 6:219-223.
- Kitzmilller, J.L., L.A. Gavin, G.D. Gin, L. Jovanovic-Peterson, E.K. Main, and W.D. Zigrang. 1991. Preconception care of diabetes. Glycemic control prevents congenital anomalies. *JAMA (J. Am. Med. Assoc.)*. 265:731-736.
- Watanabe, G., and T.H. Ingalls. 1973. Congenital malformations in the offspring of alloxan diabetic mice. *Diabetes*. 12:66-67.
- Deuchar, E.M. 1977. Embryonic malformations in rats, resulting from maternal diabetes: preliminary observations. *J. Embryol. Exp. Morphol.* 41:93-99.
- Eriksson, U.J., N.J. Lewis, and N. Freinkel. 1984. Growth retardation during early organogenesis in embryos of experimentally diabetic rats. *Diabetes*. 33:281-284.
- Freinkel, N., N.J. Lewis, S. Akazawa, S.I. Roth, and L. Gorman. 1984. The honeybee syndrome: implications of the teratogenicity of mannose in rat-embryo culture. *N. Engl. J. Med.* 310:223-230.
- Buchanan, T.A., and N. Freinkel. 1988. Fuel-mediated teratogenesis: symmetric growth retardation in the rat fetus at term after a circumscribed exposure to D-mannose during organogenesis. *Am. J. Obstet. Gynecol.* 158:663-669.
- Otani, H., O. Tanaka, R. Tatewaki, H. Naora, and T. Yoneyama. 1991. Diabetic environment and genetic predisposition as cause of congenital malformations in NOD mouse embryos. *Diabetes*. 40:1245-1250.
- Cagliero, E., H. Forsberg, R. Sala, M. Lorenzi, and U.J. Eriksson. 1993. Maternal diabetes induces increased expression of extracellular matrix components in rat embryos. *Diabetes*. 42:975-980.
- Finley, B.E., and S. Norton. 1991. Effects of hyperglycemia on mitochondrial morphology in the region of the anterior neuropore in the explanted rat embryo model: evidence for modified Reid hypothesis as a mechanism for diabetic teratogenesis. *Am. J. Obstet. Gynecol.* 165:1661-1666.
- Mouzon, S.H., P. Peraldi, F. Alengrin, and E. Van Obberghen. 1993. Alteration of phosphotyrosine phosphatase activity in tissues from diabetic and pregnant rats. *Endocrinology*. 132:67-74.
- Mouzon, S.H., M. Louizeau, and J. Girard. 1992. Functional alterations of type-I insulin-like growth factor receptor in placenta of diabetic rat. *Biochem. J.* 288:273-279.
- Akashi, M., S. Akazawa, M. Akazawa, R. Trocino, M. Hashimoto, Y. Maeda, H. Yamamoto, E. Kawasaki, H. Takino, and A. Yokota. 1991. Effect of insulin and myo-inositol on embryo growth and development during early organogenesis in streptozotocin-induced diabetic rats. *Diabetes*. 40:1574-1579.
- Eriksson, U.J., and L.A. Borg. 1991. Protection of free oxygen radicals scavenging enzymes against glucose-induced embryonic malformations in vitro. *Diabetologia*. 34:325-331.

22. Strielman, P.J., M.A. Connors, and B.E. Metzger. 1992. Phosphoinositide mechanism in developing conceptus. Effects of hyperglycemia and scyllo-inositol in rat embryo culture. *Diabetes*. 41:989-997.
23. Baker, L., R. Paddington, A. Goldman, J. Egler, and J. Moehring. 1990. Myo-inositol and prostaglandins reverse the glucose inhibition of neural tube fusion in cultured mouse embryos. *Diabetologia*. 33:593-596.
24. Saxen, L. 1987. Organogenesis of the Kidney. Cambridge University Press, New York. 173.
25. Reeves, W.H., Y.S. Kanwar, and M.G. Farquhar. 1980. Assembly of glomerular filtration surface. Differentiation of anionic sites in glomerular capillaries of rat kidney. *J. Cell Biol.* 85:735-753.
26. Clapp, W.L., and D.R. Abrahamson. 1993. Regulation of kidney organogenesis: homeobox genes, growth factors and Wilms tumor. *Curr. Opin. Nephrol. Hypertens.* 2:419-429.
27. Lelongt, B., H. Makino, T.M. Dalecki, and Y.S. Kanwar. 1988. Role of proteoglycans in renal development. *Dev. Biol.* 128:256-276.
28. Liu, Z.Z., T.M. Dalecki, N. Kashihara, E.I. Wallner, and Y.S. Kanwar. 1991. Effect of puromycin on metanephric differentiation: morphological, autoradiographic and biochemical studies. *Kidney Int.* 39:1140-1155.
29. Platt, J.L., D.M. Brown, K. Granlund, and T.R. Oegema, and D.J. Klein. 1987. Proteoglycan metabolism associated with mouse metanephric development: morphologic and biochemical effect of β -D-xyloside. *Dev. Biol.* 123:293-306.
30. Kanwar, Y.S., Z.Z. Liu, A. Kumar, J. Wada, and F.A. Carone. 1995. Cloning of mouse *c-ros* renal cDNA, its role in development and relationship to extracellular matrix glycoproteins. *Kidney Int.* 48:1646-1659.
31. Wada, J., Z.Z. Liu, K. Alvares, A. Kumar, E.I. Wallner, H. Makino, and Y.S. Kanwar. 1993. Cloning of cDNA for the α subunit of mouse insulin-like growth factor-I receptor and the role of receptor in metanephric development. *Proc. Natl. Acad. Sci. USA.* 90:10360-10364.
32. Liu, Z.Z., A. Kumar, E.I. Wallner, J. Wada, F.A. Carone, and Y.S. Kanwar. 1994. Trophic effect of insulin-like growth factor-I on metanephric development: relationship to proteoglycans. *Eur. J. Cell Biol.* 65:378-391.
33. Cagliero, E., M. Maiello, D. Boeri, S. Roy, and M. Lorenzi. 1988. Increased expression of basement membrane components in human endothelial cells cultured in high glucose. *J. Clin. Invest.* 82:735-738.
34. Kanwar, Y.S., Y. Yoshinaga, Z. Liu, E.I. Wallner, and F.A. Carone. 1992. Biosynthetic regulation of proteoglycans by aldohexoses and ATP. *Proc. Natl. Acad. Sci. USA.* 89:8621-8625.
35. Ayo, S.H., R.A. Radnik, J. Garoni, W.F. Glass, and J.A. Kreisberg. 1990. High glucose causes an increase in extracellular matrix proteins in cultured mesangial cells. *Am. J. Pathol.* 136:1339-1348.
36. Ziyadeh, F.N., K. Sharma, M. Ericksen, and G. Wolf. 1994. Stimulation of collagen gene expression and protein synthesis in murine mesangial cells by high glucose mediated by autocrine activation of transforming growth factor- β . *J. Clin. Invest.* 93:536-542.
37. Kasinath, B.S., P. Grellier, G. Ghosh Choudhury, and S.L. Abboud. 1996. Regulation of basement membrane sulfate proteoglycan, perlecan, gene expression in glomerular epithelial cells by high glucose medium. *J. Cell. Physiol.* 167:131-136.
38. Smeaton, T.C., and B.D. Eichner. 1983. Measurement of DNA with an automatic spectrophotometer. *Anal. Biochem.* 131:394-396.
39. Sanger, F., S. Nicklen, and A.R. Coulson. 1977. DNA sequencing with chain-terminating inhibitors. *Proc. Natl. Acad. Sci. USA.* 74:5463-5467.
40. Chomczynski, P., and N. Sacchi. 1987. Single-step method of RNA isolation by acid guanidinium thiocyanate-phenol-chloroform extraction. *Anal. Biochem.* 162:156-159.
41. Cohen, I.R., S. Grassel, A.D. Murdoch, and R.V. Iozzo. 1993. Structural characterization of the complete human perlecan gene and its promoter. *Proc. Natl. Acad. Sci. USA.* 90:10404-10408.
42. Dignam, J.D., R.M. Lebovitz, and R.G. Roeder. 1983. Accurate transcription initiation by RNA polymerase II in a soluble extract from isolated mammalian nuclei. *Nucleic. Acids Res.* 11:1475-1489.
43. Imagawa, M., R. Chiu, and M. Karin. 1987. Transcription factor AP-2 mediates induction by two different signal-transduction pathways: protein kinase C and cAMP. *Cell.* 51:251-260.
44. Lang, G.P., and G. Michael. 1974. D-glucose-6-phosphate and D-fructose-6-phosphate. In: *Methods of Enzymatic Analysis*. H.V. Bergmeyer, editor. Verlag Chemie GmbH, Weinheim, Germany. 1238-1242.
45. Vasan, S., X. Zhang, X. Zhang, A. Kapuriotu, J. Bernhagen, S. Teichberg, J. Basgen, D. Wagle, D. Shih, I. Terlecky, R. Bucala et al. 1996. An agent cleaving glucose-derived protein crosslinks in vitro and in vivo. *Nature (Lond.)* 382:275-278.
46. Koseki, C., D. Herzlinger, and Q. Al-Awqati. 1992. Apoptosis in metanephric development. *J. Cell Biol.* 119:1327-1333.
47. Gonzalez, K., S. McVey, J. Cunnick, I.P. Udovichenko, and D.J. Takemoto. 1994. Acridine orange differential staining of total DNA and RNA in normal and galactosemic lens epithelial cells in culture using flow cytometry. *Curr. Eye Res.* 14:269-273.
48. Nagata, M., H. Nakauchi, K.I. Nakayama, K. Nakayama, D. Loh, and T. Watanabe. 1996. Apoptosis during an early stage of nephrogenesis induces renal hypoplasia in *bcl-2*-deficient mice. *Am. J. Pathol.* 148:1601-1611.
49. Chinnaiyan, A.M., and V.M. Dixit. 1996. The cell-death machine. *Curr. Biol.* 6:555-562.
50. Ueda, N., and S.V. Shah. 1992. Endonuclease-induced DNA damage and cell death in oxidant injury to renal tubular epithelial cells. *J. Clin. Invest.* 90:2593-2597.
51. Fang, W., J.J. Rivard, J.A. Ganser, T.W. LeBien, K.A. Nath, D.L. Mueller, and T.W. Behrens, T.W. 1995. BcL-xL rescues WEHI 231 B lymphocytes from oxidant-mediated death following diverse apoptotic stimuli. *J. Immunol.* 155:66-75.
52. Nerlich, A., and E. Schleicher. 1991. Immunohistochemical localization of extracellular matrix components in human diabetic glomerular lesions. *Am. J. Pathol.* 139:889-899.
53. Roy, S., R. Sala, E. Cagliero, and M. Lorenzi. 1990. Over-expression of fibronectin induced by diabetes or high glucose: phenomenon with a memory. *Proc. Natl. Acad. Sci. USA.* 87:404-408.
54. Fukui, M., T. Nalamura, I. Ebihara, I. Shirato, Y. Tomino, and H. Koide. 1992. ECM gene expression and its modulation by insulin in diabetic rats. *Diabetes*. 41:1520-1527.
55. Setty, S., S.S. Anderson, E.A. Wayner, Y. Kim, D.O. Clegg, and E.C. Tsilibary. 1995. Glucose-induced alteration of integrin expression and function in cultured human mesangial cells. *Cell Adhesion and Communication.* 3:187-200.
56. Kanwar, Y.S., L.J. Rosenzweig, A. Linker, and M.L. Jakubowski. 1983. Decreased de novo synthesis of glomerular proteoglycans in diabetes: biochemical-autoradiographic evidence. *Proc. Natl. Acad. Sci. USA.* 80:2272-2275.
57. Wight, T.N., D.K. Heinegard, and V.C. Hascall. 1991. Proteoglycans: structure and function. In *Cell Biology of Extracellular Matrix*. E.D. Hay, editor. Plenum Publishing Corp., New York. 45-78.
58. Ruoslahti, E., and Y. Yamaguchi. 1991. Proteoglycans as modulators of growth factor activities. *Cell.* 64:867-869.
59. Furuya, S., M. Sera, R. Tohno-oka, K. Sugahara, K. Shiokawa, and Y. Hirabayashi. 1995. Elimination of heparan sulfate by heparinases induces abnormal mesodermal and neural formation in *Xenopus* embryos. *Dev. Growth Differ.* 37:337-346.
60. Kashihara, N., Y. Watanabe, H. Makino, E.I. Wallner, and Y.S. Kanwar. 1992. Selective decreased de novo synthesis of glomerular proteoglycans under the influence of reactive oxygen species (ROS). *Proc. Natl. Acad. Sci. USA.* 89:6309-6313.
61. Ayo, S.H., R. Radnik, J.A. Garoni, D.A. Troyer, and J.I. Kreisberg. 1991. High glucose increases diacylglycerol mass and activates protein kinase C in mesangial cell cultures. *Am. J. Physiol.* 261:F571-F577.
62. Wyllie, A.H. 1987. Cell death. *Int. Rev. Cytol.* 517:755-785.